Journal of Inorganic and General Chemistry
ZAAC
Zeitschrift für anorganische und allgemeine Chemie
doi.org/10.1002/zaac.202100204
ARTICLE

# Synthesis, Crystal Structures and Properties of $Ni(NCS)_2$-3-Cyanopyridine Coordination Compounds including a Ferromagnetic Layered Compound

Christoph Krebs,[a] Solveig Thiele,[a] Magdalena Ceglarska,[b] and Christian Näther*[a]

*Dedicated to Prof. Dr. Josef Breu on the occasion of his 60th birthday.*

Reactions of $Ni(NCS)_2$ and 3-cyanopyridine in different solvents lead to the formation of $Ni(NCS)_2$(3-cyanopyridine)$_4$ (**1**) already reported in the literature, $Ni(NCS)_2$(3-cyanopyridine)$_2(H_2O)_2$ (**2**), $Ni(NCS)_2$(3-cyanopyridine)$_2(CH_3OH)_2$ (**3**), $Ni(NCS)_2$(3-cyanopyridine)$_2(CH_3CN)_2$ (**4**) and $Ni(NCS)_2$(3-cyanopyridine)$_2$ (**5**). The crystal structures of **1**–**4** consist of discrete octahedral complexes, in which the thiocyanate anions, as well as the 3-cyanopyridine coligands, are only terminally N-bonded. In compound **5** the Ni cations are octahedrally coordinated and linked by pairs of thiocyanate anions into dinuclear units that are further connected into layers by single μ-1,3-bridging anionic ligands. TG-DTA measurements of the discrete complex **1** reveal that in the first step half of the coligands are emitted leading to the formation of compound **5**. In contrast, compounds **2** and **3** transform into a new crystalline phase of the same composition (**6**) upon heating that should also contain μ-1,3-bridging anionic ligands, but the outcome of this reaction strongly depends on the reaction conditions. The acetonitrile complex **4** is unstable at room temperature and decomposes into a mixture of different phases including the aqua complex **2**. Magnetic measurements of compound **5** prove a ferromagnetic transition at $T_c = 6.0$ K. This result is compared to those obtained for other thiocyanate compounds exhibiting a similar layer topology.

## Introduction

The synthesis of new coordination polymers with desired magnetic properties is an important field in coordination chemistry.[1–3] In this context, both, compounds with discrete or extended building units are of interest. The former compounds are of special importance if spin-crossover or single ion respectively single molecule magnets are to be synthesized, whereas coordination polymers are usually needed if compounds with cooperative magnetic properties like e.g. single chain magnets or ferromagnets are in the focus of investigations.[3–14] For the synthesis of the latter compounds paramagnetic metal cations must be linked by ligands that are able to mediate significant magnetic exchange and in this context, numerous compounds based on e.g. cyanides or azides are reported in the literature.[14-24]

We and others have focused on compounds based on the thiocyanate anion, which is a versatile ligand that is able to bind to metal cations in many different ways. For less chalcophilic metal cations the N-terminal coordination is preferred, while the synthesis of compounds with bridging coordination is sometimes more difficult to achieve.[25] In the majority of the latter compounds, the metal cations are octahedrally coordinated and linked into chains by μ-1,3-bridging ligands.[26–34] Depending on the actual metal coordination (all-*trans*- or *cis-cis-trans)* these chains can be linear or corrugated.[29,35–38] With other ligands, however, layered thiocyanate structures are observed, in which the metal cations are exclusively linked by single anionic ligands or in which they are linked by pairs of thiocyanate anions into dinuclear units that are further connected by single anionic ligands.[39–41]

Concerning the magnetic properties of such compounds, those based on Co(II) and Ni(II) are of special interest because in most cases the intra-layer/intra-chain magnetic exchange is ferromagnetic. For the Co(II) chain compounds either ferromagnetic or antiferromagnetic ordering is observed and the latter frequently shows single chain magnet behaviour, although a few exceptions are known.[32,42–43] For the Ni(II) chain compounds usually no magnetic ordering is observed. In contrast, Co and Ni compounds with layered thiocyanate networks show ferromagnetic ordering with critical temperatures that are significantly higher for Ni than for Co, which can be used e.g. to tune the critical temperature by preparing solid solutions.[44–46]

[a] *M. Sc. C. Krebs, B. Sc. S. Thiele, Prof. Dr. C. Näther*
*Institute of Inorganic Chemistry*
*Christian-Albrechts-University of Kiel*
*Max-Eyth-Straße 2*
*24118 Kiel*
*Germany*
*E-mail: cnaether@ac.uni-kiel.de*
[b] *M. Sc. M. Ceglarska*
*Institute of Physics, Jagiellonian University*
*Łojasiewicza 11, 30-348 Kraków*
*Poland*

Supporting information for this article is available on the WWW under https://doi.org/10.1002/zaac.202100204

*© 2021 The Authors. Zeitschrift für anorganische und allgemeine Chemie published by Wiley-VCH GmbH. This is an open access article under the terms of the Creative Commons Attribution Non-Commercial NoDerivs License, which permits use and distribution in any medium, provided the original work is properly cited, the use is non-commercial and no modifications or adaptations are made.*

In the course of our systematic work, we became interested in Ni(II) compounds with cyanopyridines as coligands, which can act as a terminal or as a bridging ligand.[47–48] Some compounds consisting of transition metal thiocyanates with 3-cyanopyridine are already reported.[49–53] For Ni only one discrete complex with the composition $Ni(NCS)_2$(3-cyanopyridine)$_4$ is known. During our investigations, we discovered some new discrete complexes with this coligand, but also a layered compound that shows a very rare topology similar to that observed in compounds with 4-acetylpyridine and ethylisonicotinate reported recently.[40–41] Both of these compounds show ferromagnetic ordering. Therefore, magnetic measurements were performed in order to verify if this could also be observed in the new 3-cyanopyridine compound.

## Results and Discussion

### *Synthesis and Characterization*

Reactions of different stoichiometric ratios of $Ni(SCN)_2$ with 3-cyanopyridine in various solvents yield five different crystalline phases (Table 1). If a ratio of 1:4 is used, IR and XRPD investigations prove that in all solvents the discrete complex $Ni(NCS)_2$(3-cyanopyridine)$_4$ (**1**) is obtained, which is already reported in the literature (Figure S1 and S2).[53] Lowering the $Ni(NCS)_2$:3-cyanopyridine ratio to 1:2 leads to the formation of new crystalline phases **2**–**5**, of which only the one obtained from acetonitrile was pure. Compound **2** can be obtained in the pure form if the 3-cyanopyridine content is further reduced, while **3** is available as a pure phase if the synthesis is carried out in dry methanol (Table 1).

For compounds **2**–**4** elemental analyses indicate that compounds with the composition $Ni(NCS)_2$(3-cyanopyridine)$_2$(L)$_2$ (L = water, methanol and acetonitrile) were obtained, even if for **4** deviating results were observed, indicating that this compound is unstable at room temperature. In the IR spectra the CN stretching vibrations of the thiocyanate anions and the cyano group are observed at 2107 and 2242 cm$^{-1}$ for **2**, at 2097 and 2242 cm$^{-1}$ for **3** and 2074 and 2240 cm$^{-1}$ for **4**, indicating that the thiocyanate anions are only terminally bonded and that the cyano group of the coligand is not involved in the metal coordination (Table 2 and Figures S3-S5). The value for the CN stretch of the anionic ligands for **2** and **3** is at the borderline to that expected for μ-1,3-bridging ligands, but this value is usually shifted to higher wavenumbers if O-donor coligands are coordinated to the metal centers. Therefore, it can be assumed that solvato complexes formed, in which the Ni(II) cations are octahedrally coordinated by two thiocyanate anions, two 3-cyanopyridine ligands and two water, methanol or acetonitrile molecules.

For compound **5**, the CN stretching vibration is observed at 2119 cm$^{-1}$ for the anionic ligand and at 2236 cm$^{-1}$ for the cyano group, which proves that the metal cations are linked by only μ-1,3-bridging thiocyanate anions (Figure S6).

For all compounds, single crystals were obtained and characterized by single crystal X-ray diffraction (Table S1).

**Table 1.** Compounds that are obtained if different ratios between $Ni(NCS)_2$ and 3-cyanopyridine react in water, methanol, ethanol and acetonitrile. Unknown complexes are marked with *.

| | Ratio between $Ni(NCS)_2$ and 3-cyanopyridine | | | |
|---|---|---|---|---|
| solvent | 1:4 | 1:2 | 1:1 | 2:1 |
| water | **1** | **2** + **1** | **2** | **2** |
| methanol | **1** | **3** + **2** | **3** + **2** | **3** + **2** |
| ethanol | 1 | **5** + **1** | **5** | * |
| acetonitrile | **1** | **4** | $Ni(SCN)_2$ | $Ni(SCN)_2$ |

**Table 2.** Values of the CN stretching vibration (cm$^{-1}$) for the thiocyanate anion and the cyano group of the coligand observed in the IR spectra of compounds **1**–**5**.

| | **1** | **2** | **3** | **4** | **5** |
|---|---|---|---|---|---|
| Thiocyanate anion | 2080 | 2107 | 2097 | 2074 | 2119 |
| Cyano group | 2234 | 2242 | 2242 | 2240 | 2236 |

### *Crystal structures*

### *Crystal structures of the discrete complexes 1–4*

The crystal structure of $Ni(NCS)_2$(3-cyanopyridine)$_4$ (**1**) is already reported in the literature but was measured at room temperature. For better comparability with the other structures, it was additionally measured at 100 K. This compound crystallizes in the orthorhombic space group $Pna2_1$ with Z = 4 and all atoms in general positions. This structure consists of discrete complexes, in which the Ni(II) cations are octahedrally coordinated by two terminal N-bonded thiocyanate anions and four 3-cyanopyridine coligands that are connected *via* the pyridine N atoms to the metal centers (Figure S7). The Ni–N bond distances to the coligands are significantly longer than those to the anionic ligands and range between 2.1383(15) and 2.1766(15) Å (Table S2). From the bond angles it is obvious that the octahedra are slightly distorted, which is also obvious from the octahedral angle variance value of 5.3684 and the mean octahedral quadratic elongation of 1.0034 (Table S2).

Compounds **2**–**4** form solvato complexes, in which the Ni cations are always octahedrally coordinated by two anionic ligands, two 3-cyanopyridine coligands and two water, methanol, or acetonitrile molecules (Figure 1) each.

Compounds **2** and **3** crystallize in the monoclinic space groups $P2_1/c$ (**2**) and $P2_1/n$ (**3**), whereas compound **4** crystallizes in the triclinic space group $P\bar{1}$. For all three compounds the asymmetric unit consists of one thiocyanate anion and one 3-cyanopyridine coligand in general positions and one Ni(II) cation which is located on an inversion center. In compound **2**, the Ni–N bond lengths to the thiocyanate anion are slightly longer than those in **3** and **4**, whereas those to the 3-cyanopyridine coligand are significantly elongated in compound **4** (Table S3-S5). Compared to compound **3**, the Ni–O bond lengths are significantly shortened in **2**, indicating a


© 2021 The Authors. Zeitschrift für anorganische und allgemeine Chemie published by Wiley-VCH GmbH.

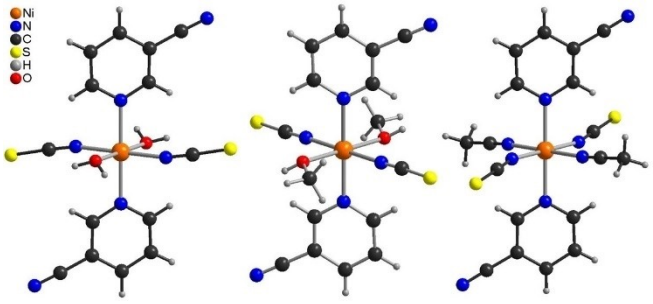


**Figure 1.** View of the discrete complexes in the crystal structure of **2** (left), **3** (middle) and **4** (right). ORTEP plots of compounds **1–4** are given in Figures S7-S10.

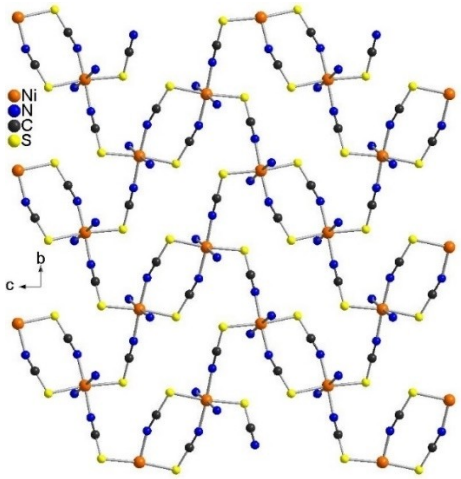


**Figure 2.** Crystal structure of compound **5** with a view of the thiocyanate network along the crystallographic *a*-axis. Only the N atoms of the 3-cyanopyridine ligands are shown - An ORTEP plot can be found in Figure S14 and a view of the layers with the 3-cyanopyridine coligands in Figure S15.

stronger interaction (Table S3 and S4). In all three complexes, the octahedra deviate from the ideal geometry with the strongest distortion being in the methanol complex **3**. This is also obvious from the octahedral angle variance and the angular distortion (Table 3).

In the crystal structure of compound **2**, the discrete complexes are linked by pairs of O–H···S hydrogen bonds into chains that are further connected into a 3D network by C–H···S hydrogen bonding (Figure S11). Bond lengths and angles indicate a relatively strong interaction (Table S6). O–H···S hydrogen and C–H···S hydrogen bonding is also found in compound **3**, but in this case, only layers are formed (Figure S12 and Table S7). In contrast, for compound **4** only weak C–H···S and C–H···N interactions are found, which link the discrete complexes into a 3D network (Figure S13 and Table S8).

### *Crystal structure of the layered compound 5*

Compounds **5** crystallizes in the monoclinic space group $P2_1/c$ with Z = 4 and all atoms in general positions. The Ni(II) cations are octahedrally coordinated by two N- and two S-bonding thiocyanate anions and two 3-cyanopyridine ligands in an all-*trans* configuration (Figure S14). Bond lengths and angles correspond to literature values and from the bonding angles it is obvious that the octahedra are slightly distorted (Table S9). Each two Ni(II) cations are linked by pairs of μ-1,3-bridging thiocyanate anions into dinuclear units that are further linked by single anionic ligands into layers that are parallel to the *b*-/*c*-plane (Figure 2).

It is noted that the topology of the thiocyanate network is comparable to that in $[Ni(NCS)_2(4\text{-acetylpyridine})_2]_n$[41] and in $[Ni(NCS)_2(ethylisonicotinate)_2]_n$[40] recently reported.

**Table 3.** Octahedral angle variance and angular distortion of compounds **2–4**.

| | 2 | 3 | 4 |
|---|---|---|---|
| octahedral angle variance | 1.6714 | 4.1910 | 1.5271 |
| mean octahedral quadratic elongation | 1.0008 | 1.0018 | 1.0012 |

Between the layers, no pronounced intermolecular interactions are found. There are only some intra-layer C–H···S and C–H···N hydrogen bonds, but from the distances and angles it is obvious that these represent only very weak interactions (Table S10).

Based on all crystal structures, XRPD patterns were calculated and compared with the experimental patterns, which prove that compounds **2–5** were obtained as pure samples (Figure S16-S19).

### *Thermoanalytical investigations for compounds 1–4*

In order to examine whether 3-cyanopyridine-deficient compounds are accessible by thermal decomposition, compounds **1–4** were investigated by TG-DTA measurements (Figure S20–S23).

When compound **1** is heated with 1 °C/min two well resolved mass losses are observed which are accompanied by endothermic events in the DSC curve (Figure 3 and Figure S20). The experimental mass losses of 33.8 % in the first and 36.0 % in the second step are in good agreement with the calculated value for the removal of two 3-cyanopyridine ligands in each step ($\Delta m_{calc.} = 35.2\,\%$).

The measurement was repeated and the residue isolated after the first mass loss was investigated by XRPD, which proved that the layer compound **5** formed (Figure S24).

TG-DTA measurements on compound **2** show a more complicated behaviour as three mass steps are observed, of which the first and third are endothermic, while the second is exothermic (Figure 3 and Figure S21). The experimental mass loss in the first TG step is in good agreement with that calculated for the emission of the water molecules ($\Delta m_{calc.} = 8.6\,\%$), whereas the mass loss in the third TG step roughly


© 2021 The Authors. Zeitschrift für anorganische und allgemeine Chemie published by Wiley-VCH GmbH.

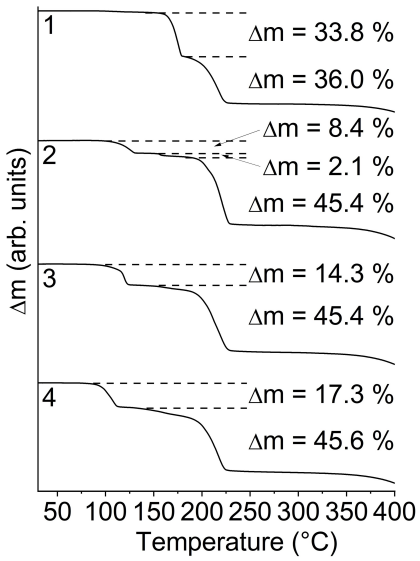


**Figure 3.** TG curves for compounds **1**–**4** measured with 1 °C/min.

corresponds to the removal of the remaining 3-cyanopyridine ligands ($\Delta m_{calc.}$ = 49.7 %). The occurrence of the second TG step is difficult to explain because it is too small to correspond to the formation of a compound with a reasonable composition. XRPD measurements of the residue formed in the first TG step reveal that a new crystalline phase (**6**) contaminated with small amounts of compound **5** has formed (Figure S24). XRPD investigations of the residue isolated after the second mass loss show that compound **6** has formed exclusively (Figure S25). For compound **6** elemental analysis indicates a composition that is identical to that of **5** and IR investigations show that the CN-stretching vibration of the cyano group is observed at 2236 $cm^{-1}$, indicating that the cyano group is still not involved in metal coordination. For the CN stretch of the thiocyanate anions, one band is observed at 2107 $cm^{-1}$, which proves the presence of μ-1,3-bridging anionic ligands **6** (Figure S26).

For the methanol complex **3** two mass losses are observed, of which the first corresponds to the removal of the methanol molecules ($\Delta m_{calc.}$ = 14.3 %) and the second to the emission of two 3-cyanopyridine ligands ($\Delta m_{calc.}$ = 46.6 %) (Figure 3 and Figure S27). As already observed for the aqua complex **2** the residue formed after the first mass loss corresponds to a mixture of **5** and **6** but in this case, the amount of **5** is more significant (Figure S27).

Finally, a TG-DTA measurement of the acetonitrile complex **4** reveals two mass steps. In the first step, two acetonitrile molecules are removed ($\Delta m_{calc.}$ = 17.6 %), whereas the second step can be assigned to the removal of two 3-cyanopyridine ligands ($\Delta m_{calc.}$ = 44.8 %). It is noted that this complex is unstable and immediately decomposes at room temperature and that the residue is hygroscopic leading to compound **2** as the major phase (Figure S28). Therefore, no further investigations were performed.

As mentioned above, the TG-DTA curve of the aqua complex **2** shows a more complex behaviour because the two distinct mass losses, as well as the exothermic signal after the first mass loss, are surprising and difficult to understand. The exothermic event might be traced back to the crystallization of a new phase starting from the melt or an amorphous intermediate phase. Even if the former is unlikely because no endothermic peak that indicates melting is visible, compound **2** was investigated by thermomicroscopy (Figure 4).

Upon heating, the water removal takes place starting at about 135 °C. The crystal starts cracking and the parts that have already been transformed appear black, which originates from different orientations of the domains of the product phase (Figure 4). All these findings are in agreement with a first order transition that proceeds *via* nucleation and growth of a new phase. There are no indications that any phase melts in the beginning and crystallizes upon further heating. Measurements using temperature-dependent XRPD show that compound **2** starts to decompose at about 110 °C and an amorphous phase is obtained that crystallizes with further heating (Figure 5). Therefore, the exothermic peak observed in the TG-DTA measurement of **2** can be traced back to the crystallization of an intermediate amorphous phase.

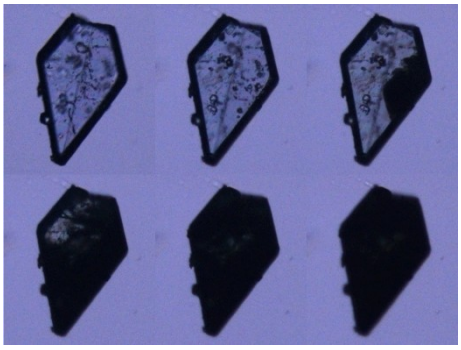

**Figure 4.** Microscopic images of a crystal of compound **2** at different temperatures (top left to bottom right: 40 °C, 130 °C, 135 °C, 140 °C, 150 °C, 190 °C).

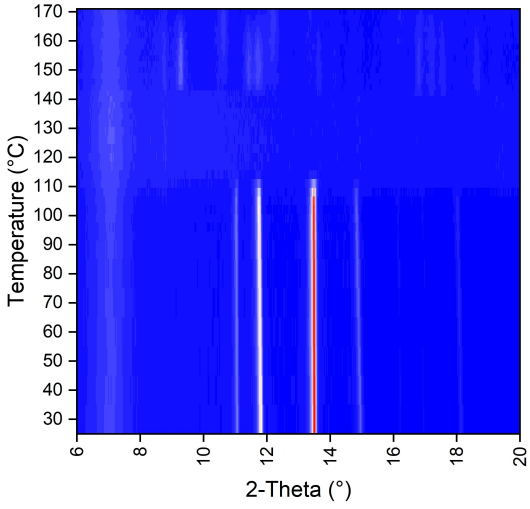


**Figure 5.** XRPD pattern of compound **2** as function of temperature.


© 2021 The Authors. Zeitschrift für anorganische und allgemeine Chemie published by Wiley-VCH GmbH.

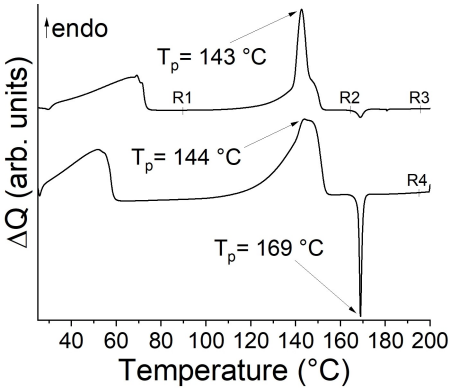


**Figure 6.** DSC curves of compound **2** measured with 10 °C/min in an almost closed (top) and an open crucible (bottom). Residues were isolated at four temperatures (R1, R2, R3 and R4).

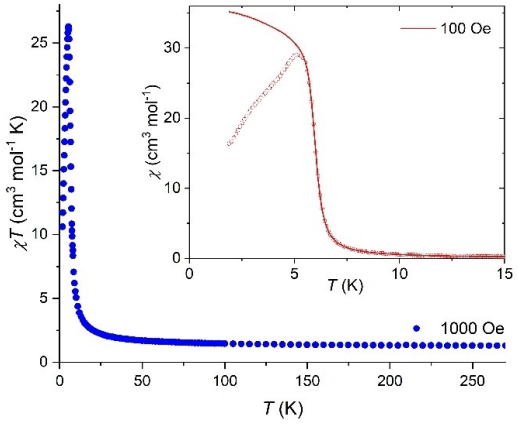


**Figure 7.** Temperature dependency of magnetic susceptibility, $\chi$, measured at 1 kOe for **5**, presented as a $\chi T$ product. Inset: Zero-field cooled (points) and field cooled (line) susceptibility measured at 100 Oe for **5**.

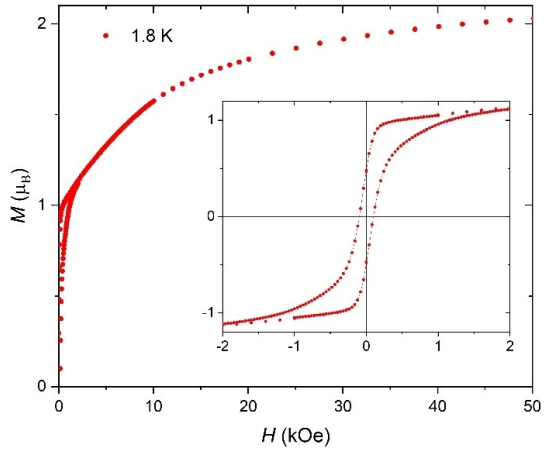


**Figure 8.** The magnetization curve measured for **5** from 50 kOe to 0 at 1.8 K. Inset: Low field magnetic hysteresis loop.

It is noted that a similar temperature-dependent XRPD measurement on compound **3** also shows decomposition into an amorphous phase that does not crystallize when further heated (Figure S29).

Additional DSC measurements on compound **2** show a broad endothermic peak between 40 and 80 °C, suggesting this sample was not completely dry. This is supported by the fact that the residue isolated after this event matches with compound **2**. (Figure S30). However, the removal of the coordinated water molecules occurs at about 143 °C, which is slightly higher than the value observed in the TG-DTA measurement (Figure 6).

Surprisingly, in contrast to the TG-DTA measurements, only a very weak exothermic signal is observed after the removal of the coordinated water molecules (Figure 6: top). As with the TG measurements of **2**, XRPD investigations prove that the residue isolated before the exothermic event is contaminated with a small amount of **5**, which is not the case after this event (Figure S30 and S31).

This could be due to the fact that the TG measurement was performed with open crucibles, while an Al dish with a very small hole was used for the DSC measurement, which means that the reaction takes place under a self-generated atmosphere. Therefore, it can be assumed that in the TG measurement the water removal is much faster, leading to the formation of an amorphous phase. To prove this assumption a second DSC measurement was performed using an Al pan with a significantly larger hole and in this case, the exothermic peak is clearly visible (Figure 6: bottom). To conclude, the TG measurement was repeated using a crucible with a cap with a small hole, which resulted in the absence of the exothermic peak (Figure S32).

What might be difficult to explain is the fact that in the TG measurement of compound **2** a second mass loss occurs after water removal. It could be that a small amount of water is incorporated in the amorphous phase that is released during crystallization, but the IR spectrum of the residue obtained after the first mass loss indicates that all water has already been removed. Alternatively, a very small amount of the 3-cyanopyridine ligand can be vaporized in the amorphous phase but this is difficult to verify.

### *Magnetic measurements*

The magnetic susceptibilities of **5** measured at 1 kOe is presented in Figure 7. The $\chi T$ value at 270 K is equal to 1.30 $cm^3$·K/mol which is common for compounds containing Ni(II) ions (spin $S=1$) and corresponds to $g=2.28$. The $\chi T$ product increases with decreasing temperature down to 5.5 K indicating ferromagnetic intralayer interactions. The zero-field and field cooled susceptibilities (Figure 7, inset) measured at 100 Oe differ below 5.5 K. The fc curve keeps increasing with decreasing temperature and approaches saturation at 1.9 K, which points to ferromagnetic ordering. The critical temperature $T_c$ was determined from $d\chi/dT$ for $\chi$ measured at 100 Oe and is equal to 6.0 K. A similar behavior was previously


© 2021 The Authors. Zeitschrift für anorganische und allgemeine Chemie published by Wiley-VCH GmbH.

observed for other layered compounds like e.g. $Ni(NCS)_2$(4-acetylpyridine)$_2$, with $T_c$ equal to 8.0 K[45] and $Ni(NCS)_2$(ethylisonicotinate)$_2$, with $T_c$ equal to 8.7 K.[40]

The magnetization curve measured at 1.8 K is shown in Figure 8. At 50 kOe the magnetization reaches 2.03 $\mu_B$, but it is still not saturated. This is typical for coordination compounds with Ni(II) ions.[35] The corresponding hysteresis loop (Figure 8., inset) has coercivity around 100 Oe.

## Conclusions

In this contribution, several new coordination compounds based on $Ni(NCS)_2$ and 3-cyanopyridine were presented. Most of them consist of discrete complexes but in one of them, the nickel cations are linked by double and single μ-1,3-bridging thiocyanate anions into layers. This compound can also be obtained by thermal decomposition of $Ni(NCS)_2$(3-cyanopyridine)$_4$ reported in the literature, whereas the removal of the water or methanol molecules from the corresponding solvato complexes leads to the formation of a different crystalline phase with the same composition as observed for the layered compound **5**.

Magnetic measurements on compound **5** reveal dominating ferromagnetic interactions and at 6.0 K ferromagnetic ordering is observed. Interestingly, ferromagnetic ordering was also observed for $Ni(NCS)_2$(4-acetylpyridine)$_2$, and $Ni(NCS)_2$(ethylisonicotinate)$_2$, which are already reported in the literature and show the same layer topology as **5**, indicating that this magnetic behaviour is common for this type of layer structure. For these two compounds mixed crystals with the corresponding Co(II) compound can be prepared which allows tuning the critical temperature of the ferromagnetic transition in this class of compounds. To investigate if this can also be done with 3-cyanopyridine as a ligand the corresponding Co(II) compound would be needed. This compound is unknown and therefore, its synthesis and magnetic behaviour will be the subject of further investigations.

## Experimental Section

### General

$Ba(SCN)_2 \cdot 3H_2O$ and 3-cyanopyridine were purchased from Alfa Aesar. $NiSO_4 \cdot 6H_2O$ was purchased from Merck. $Ni(NCS)_2$ was synthesized by the reaction of equimolar amounts of $NiSO_4 \cdot 6H_2O$ and $Ba(NCS)_2 \cdot 3H_2O$ in water. The resulting white precipitate of $BaSO_4$ was filtered off and the solvent was removed from the filtrate under reduced pressure. The purity was checked by XRPD and TG-DTA. All solvents were used without further purification.

### Synthesis of $Ni(NCS)_2$(3-cyanopyridine)$_4$ (1)

$Ni(NCS)_2$ (1.0 mmol, 174.9 mg) and 3-cyanopyridine (4.0 mmol, 416.4 mg) were mixed in 2.0 mL MeOH. The mixture was stirred for three days, the precipitate was filtered off and dried in air. Compound **1** consists of a light blue crystalline powder. Elemental analysis for $C_{26}H_{16}N_{10}NiS_2$ (591.3020 g/mol): C 52.81, H 2.73, N 23.69, S 10.85. Found: C 51.67, H 2.91, N 23.44, S 11.63. For the preparation of single crystals, $Ni(NCS)_2$ (0.2 mmol, 35.0 mg) and 3-cyanopyridine (0.8 mmol, 83.3 mg) were mixed in 0.75 mL methanol. The filtrate was stored at room temperature and single crystals were obtained within 4 d.

### Synthesis of $Ni(NCS)_2$(3-cyanopyridine)$_2(H_2O)_2$ (2)

For the synthesis of compound **2**, a mixture of $Ni(NCS)_2$ (1.0 mmol, 174.9 mg) and 3-cyanopyridine (1.0 mmol, 104.1 mg) in 2.0 mL $H_2O$ was stirred for two days, the precipitate was filtered off and dried in air. A green crystalline powder was obtained. Elemental analysis for $C_{14}H_{12}N_6NiO_2S_2$ (419.1103 g/mol): C 40.12, H 2.89, N 20.05, S 15.30. Found: C 39.66, H 2.99, N 19.86, S 15.82. Single crystals of this compound were obtained after a mixture of $Ni(NCS)_2$ (0.2 mmol, 35.0 mg) and 3-cyanopyridine (0.4 mmol, 41.6 mg) were added together in 0.75 mL of demin. water. The filtrate was stored at room temperature and single crystals were obtained within 4 d.

### Synthesis of $Ni(NCS)_2$(3-cyanopyridine)$_2(CH_3OH)_2$ (3)

After stirring a mixture of $Ni(NCS)_2$ (1.0 mmol, 174.9 mg) and 3-cyanopyridine (1.0 mmol, 104.1 mg) in 2.0 mL dry methanol for two days the residue was filtered off and a light green crystalline powder was obtained. Elemental analysis for $C_{16}H_{16}N_6NiO_2S_2$ (447.1640 g/mol): C 42.98, H 3.61, N 18.79, S 14.34. Found: C 41.84, H 3.58, N 18.91, S 14.95. For the preparation of single crystals, $Ni(NCS)_2$ (0.2 mmol, 35.0 mg) and 3-cyanopyridine (0.1 mmol, 10.4 mg) were mixed in 0.75 mL methanol. The filtrate was stored at room temperature and single crystals were obtained within 4 d.

### Synthesis of $Ni(NCS)_2$(3-cyanopyridine)$_2(CH_3CN)_2$ (4)

After stirring a mixture of $Ni(NCS)_2$ (1.0 mmol, 174.9 mg) and 3-cyanopyridine (2.0 mmol, 208.2 mg) in 2.0 mL dry acetonitrile for two days the precipitate was filtered off and a green crystalline powder was obtained. For the preparation of single crystals, $Ni(NCS)_2$ (0.2 mmol, 35.0 mg) and 3-cyanopyridine (0.4 mmol, 41.6 mg) were mixed in 0.75 mL dry acetonitrile. The filtrate was stored at room temperature and single crystals were obtained within 4 d. It is noted that this compound immediately decomposes at room-temperature and therefore, several elemental analyses did not lead to consistent results.

### Synthesis of $[Ni(NCS)_2$(3-cyanopyridine)$_2]_n$ (5)

A green crystalline powder was obtained by stirring $Ni(NCS)_2$ (1 mmol, 174.9 mg) and 3-cyanopyridine (1 mmol, 104.1 mg) in 2.0 mL ethanol for two days. The filtered off residue was dried in air. Elemental analysis for $C_{14}H_8N_6NiS_2$ (383.0797 g/mol): C 43.90, H 2.10, N 21.94, S 16.74. Found: C 42.89, H 2.30, N 21.63, S 15.95. Single crystals were prepared by heating $Ni(NCS)_2$ (0.1 mmol, 17.5 mg) and 3-cyanopyridine (0.2 mmol, 20.8 mg) in 0.5 mL ethanol up to 75 °C. The solution was allowed to cool to room temperature and single crystals were obtained after 4 d.

### Single crystal structure analysis

Data collection was performed using an XtaLAB Synergy, Dualflex, HyPix diffractometer from Rigaku with Cu–Kα radiation. The structures were solved with SHELXT[54] and structure refinement was performed against $F^2$ using SHELXL-2016.[55] The C–H hydrogen atoms were positioned with idealized geometry (methyl H atoms allowed to rotate but not to tip) and were refined isotropically with


© 2021 The Authors. Zeitschrift für anorganische und allgemeine Chemie published by Wiley-VCH GmbH.

$U_{iso}$ (H) = 1.2 $U_{eq}$ (C) (1.5 for methyl H atoms) using a riding model. The O–H hydrogen atoms were located in the difference map, their bond lengths were set to ideal values and finally, they were refined isotropically with $U_{iso}$ (H) = 1.5 $U_{eq}$ (O) using a riding model.

Selected crystal data and details of the structure refinements are given in Table S1.

CCDC-2088746 (**1**), CCDC-2088745 (**2**), CCDC-2088748 (**3**), CCDC-2088749 (**4**) and CCDC-2088747 (**5**) contain the supplementary crystallographic data for this paper. These data can be obtained free of charge from the Cambridge Crystallographic Data Centre *via* http://www.ccdc.cam.ac.uk/data_request/cif.

### *Other physical measurements*

Elemental analysis was performed with a vario MICRO cube from Elementar Analysensysteme GmbH.

IR spectra were recorded at RT on a Bruker Vertex70 FT-IR spectrometer using a broadband spectral range extension VERTEX FM for full mid and far IR.

For TG-DTA measurements a STA-PT1000 thermobalance from Linseis was used. Measurements were performed in $Al_2O_3$ crucibles and under a dynamic nitrogen atmosphere. The instruments were calibrated using standard referencing materials and corrected for buoyancy.

The XRPD measurements for the characterization of all samples were performed with a Stoe Transmission Powder Diffraction System (STADI P) with Cu-$K_{\alpha1}$ radiation and a Dectris Mythen 1 K detector with a Johann-type-Ge(111) monochromator from STOE & CIE.

Temperature-resolved powder diffraction was carried out on a Panyalytical X'Pert Pro MPD diffractometer equipped with Cu-$K_{\alpha}$ radiation and a PIXcel 1D detector and an Anton Paar HTK 1200 N high temperature chamber under He (99.999 %) atmosphere. The temperature was increased/decreased at a rate of 10 K/min, the data collection time was ~15 min. per pattern.

The magnetic measurements were conducted using a Quantum Design Magnetic Properties Measurement System 5 XL. The powder sample was packed into a gelatine capsule, a small amount of nujol was added. The results were corrected for diamagnetism of the capsule, the nujol and the sample.

## Acknowledgements

This project was supported by the State of Schleswig-Holstein. Open access funding enabled and organized by Projekt DEAL.

## Conflict of Interest

The authors declare no conflict of interest.

**Keywords:** coordination polymer · nickel thiocyanate · crystal structure · thermal properties · ferromagnet

[1] J. Ferrando-Soria, J. Vallejo, M. Castellano, J. Martínez-Lillo, E. Pardo, J. Cano, I. Castro, F. Lloret, R. Ruiz-García, M. Julve, *Coord. Chem. Rev.* **2017**, *339*, 17–103.
[2] Q. Yue, E.-Q. Gao, *Coord. Chem. Rev.* **2019**, *382*, 1–31.
[3] S. G. McAdams, A.-M. Ariciu, A. K. Kostopoulos, J. P. S. Walsh, F. Tuna, *Coord. Chem. Rev.* **2017**, *346*, 216–239.
[4] G. A. Craig, M. Murrie, *Chem. Soc. Rev.* **2015**, *44*, 2135–2147.
[5] A. K. Bar, C. Pichon, J.-P. Sutter, *Coord. Chem. Rev.* **2016**, *308, Part 2*, 346–380.
[6] S. Dhers, H. L. C. Feltham, S. Brooker, *Coord. Chem. Rev.* **2015**, *296*, 24–44.
[7] K. Liu, W. Shi, P. Cheng, *Coord. Chem. Rev.* **2015**, *289–290*, 74–122.
[8] H. L. Sun, Z. M. Wang, S. Gao, *Coord. Chem. Rev.* **2010**, *254*, 1081–1100.
[9] M. Murrie, *Chem. Soc. Rev.* **2010**, *39*, 1986–1995.
[10] M. Böhme, W. Plass, *Chem. Sci.* **2019**, *10*, 9189–9202.
[11] H. Naggert, J. Rudnik, L. Kipgen, M. Bernien, F. Nickel, L. M. Arruda, W. Kuch, C. Näther, F. Tuczek, *J. Mater. Chem. C* **2015**, *3*, 7870–7877.
[12] E. V. Peresypkina, A. M. Majcher, M. Rams, K. E. Vostrikova, *Chem. Commun.* **2014**, *50*, 7150–7153.
[13] M. Rams, E. V. Peresypkina, V. S. Mironov, W. Wernsdorfer, K. E. Vostrikova, *Inorg. Chem.* **2014**, *53*, 10291–10300.
[14] S. Chorazy, M. Rams, A. Hoczek, B. Czarnecki, B. Sieklucka, S. Ohkoshi, R. Podgajny, *Chem. Commun.* **2016**, *52*, 4772–4775.
[15] Y.-F. Zeng, X. Hu, F.-C. Liu, X.-H. Bu, *Chem. Soc. Rev.* **2009**, *38*, 469–480.
[16] J. Cernák, M. Orendác, I. Potocnák, J. Chomic, A. Orendácová, J. Skorsepa, A. Feher, *Coord. Chem. Rev.* **2002**, *224*, 51–66.
[17] J. Ribas, A. Escuer, M. Monfort, R. Vicente, R. Cortés, L. Lezama, T. Rojo, *Coord. Chem. Rev.* **1999**, *193–195*, 1027–1068.
[18] S. Tanase, J. Reedijk, *Coord. Chem. Rev.* **2006**, *250*, 2501–2510.
[19] C. S. Hong, J. E. Koo, S. K. Son, Y. S. Lee, Y. S. Kim, Y. Do, *Chem. Eur. J.* **2001**, *7*, 4243–4252.
[20] C. Rajnák, Ľ. Dlháň, J. Moncol, J. Titiš, R. Boča, *Dalton Trans.* **2018**, *47*, 15745–15750.
[21] B. Nowicka, M. Reczynski, M. Rams, W. Nitek, J. Zukrowski, C. Kapusta, B. Sieklucka, *Chem. Commun.* **2015**, *51*, 11485–11488.
[22] B. Nowicka, T. Korzeniak, O. Stefańczyk, D. Pinkowicz, S. Chorąży, R. Podgajny, B. Sieklucka, *Coord. Chem. Rev.* **2012**, *256*, 1946–1971.
[23] B. Nowicka, M. Heczko, M. Rams, M. Reczyński, B. Gaweł, W. Nitek, B. Sieklucka, *Eur. J. Inorg. Chem.* **2017**, *2017*, 99–106.
[24] M. Magott, O. Stefańczyk, B. Sieklucka, D. Pinkowicz, *Angew. Chem. Int. Ed.* **2017**, *56*, 13283–13287; *Angew. Chem.* **2017**, *129*, 13468–13472.
[25] C. Näther, S. Wöhlert, J. Boeckmann, M. Wriedt, I. Jess, *Z. Anorg. Allg. Chem.* **2013**, *639*, 2696–2714.
[26] Y. P. Prananto, A. Urbatsch, B. Moubaraki, K. S. Murray, D. R. Turner, G. B. Deacon, S. R. Batten, *Aust. J. Chem.* **2017**, *70*, 516–528.
[27] J. Palion-Gazda, B. Machura, F. Lloret, M. Julve, *Cryst. Growth Des.* **2015**, *56*, 2380–2388.
[28] E. Shurdha, C. E. Moore, A. L. Rheingold, S. H. Lapidus, P. W. Stephens, A. M. Arif, J. S. Miller, *Inorg. Chem.* **2013**, *52*, 10583–10594.
[29] A. Datta, P.-H. Liu, J.-H. Huang, E. Garribba, M. Turnbull, B. Machura, C.-L. Hsu, W.-T. Chang, A. Pevec, *Polyhedron* **2012**, *44*, 77–87.
[30] X.-Y. Wang, B.-L. Li, X. Zhu, S. Gao, *Eur. J. Inorg. Chem.* **2005**, 3277–3286.
[31] G. Yang, Q. Zhang, X.-P. Zhang, Y. Zhu, N. Seik Weng, *J. Chem. Res.* **2007**, 384–386.

 © 2021 The Authors. Zeitschrift für anorganische und allgemeine Chemie published by Wiley-VCH GmbH.

[32] A. Jochim, M. Rams, M. Böhme, T. Lohmiller, M. Ceglarska, A. Schnegg, W. Plass, C. Näther, *Inorg. Chem.* **2020**, *59*, 8971–8982.
[33] J. Werner, Z. Tomkowicz, M. Rams, S. G. Ebbinghaus, T. Neumann, C. Näther, *Dalton Trans.* **2015**, *44*, 14149–14158.
[34] J. Werner, M. Rams, Z. Tomkowicz, C. Näther, *Dalton Trans.* **2014**, *43*, 17333–17342.
[35] A. Jochim, M. Rams, T. Neumann, C. Wellm, H. Reinsch, G. M. Wójtowicz, C. Näther, *Eur. J. Inorg. Chem.* **2018**, *2018*, 4779–4789.
[36] M. Böhme, A. Jochim, M. Rams, T. Lohmiller, S. Suckert, A. Schnegg, W. Plass, C. Näther, *Inorg. Chem.* **2020**, *59*, 5325–5338.
[37] Y. Jin, Y.-X. Che, J.-M. Zheng, *J. Coord. Chem.* **2007**, *60*, 2067–2074.
[38] J. M. Shi, J. N. Chen, C. J. Wu, J. P. Ma, *J. Coord. Chem.* **2007**, *60*, 2009–2013.
[39] J. Werner, Z. Tomkowicz, T. Reinert, C. Näther, *Eur. J. Inorg. Chem.* **2015**, *2005*, 3066–3075.
[40] S. Suckert, M. Rams, M. Böhme, L. S. Germann, R. E. Dinnebier, W. Plass, J. Werner, C. Näther, *Dalton Trans.* **2016**, *45*, 18190–18201.
[41] J. Werner, T. Runčevski, R. Dinnebier, S. G. Ebbinghaus, S. Suckert, C. Näther, *Eur. J. Inorg. Chem.* **2015**, *2015*, 3236–3245.
[42] M. Rams, A. Jochim, M. Böhme, T. Lohmiller, M. Ceglarska, M. M. Rams, A. Schnegg, W. Plass, C. Näther, *Chem. Eur. J.* **2020**, *26*, 2837–2851.
[43] M. Rams, Z. Tomkowicz, M. Böhme, W. Plass, S. Suckert, J. Werner, I. Jess, C. Näther, *Phys. Chem. Chem. Phys.* **2017**, *19*, 3232–3243.
[44] T. Neumann, M. Rams, C. Wellm, C. Näther, *Cryst. Growth Des.* **2018**, *18*, 6020–6027.
[45] C. Wellm, M. Rams, T. Neumann, M. Ceglarska, C. Näther, *Cryst. Growth Des.* **2018**, *18*, 3117–3123.
[46] C. Wellm, A. M. Majcher-Fitas, M. Rams, C. Näther, *Dalton Trans.* **2020**, *49*, 16707–16714.
[47] M. Heine, L. Fink, M. U. Schmidt, *CrystEngComm* **2018**, *20*, 7556–7566.
[48] H. Zhao, A. Bodach, M. Heine, Y. Krysiak, J. Glinnemann, E. Alig, L. Fink, M. U. Schmidt, *CrystEngComm* **2017**, *19*, 2216–2228.
[49] J. V. Handy, G. Ayala, R. D. Pike, *Inorg. Chim. Acta* **2017**, *456*, 64–75.
[50] A. Jochim, I. Jess, C. Näther, *Z. Anorg. Allg. Chem.* **2019**, *645*, 212–218.
[51] A. Jochim, I. Jess, C. Näther, *Z. Naturforsch. B* **2020**, *75*, 163–172.
[52] S. Diehr, S. Wohlert, J. Boeckmann, C. Nather, *Acta Crystallogr.* **2011**, *E67*, m1898.
[53] M. L. Kilkenny, L. R. Nassimbeni, *Dalton Trans.* **2001**, 3065–3068.
[54] G. M. Sheldrick, *Acta Crystallogr.* **2015**, *A71*, 3–8.
[55] G. M. Sheldrick, *Acta Crystallogr.* **2015**, *C71*, 3–8.

Manuscript received: June 11, 2021
Revised manuscript received: July 7, 2021
Accepted manuscript online: July 9, 2021

 © 2021 The Authors. Zeitschrift für anorganische und allgemeine Chemie published by Wiley-VCH GmbH.